

1 **Clinically-Applicable Optical Imaging Technology for Body Size and**
2 **Shape Analysis: Comparison of Systems Differing in Design**

3
4 Brianna Bourgeois^{1,2}, Bennett K. Ng^{3,4}, Dustin Latimer^{1,2}, Casey R Stannard², Laurel Romeo²,
5 Xin Li², John A. Shepherd³, Steven B. Heymsfield^{1,2}

6 ¹Pennington Biomedical Research Center, Baton Rouge, Louisiana, USA; ²Louisiana State
7 University, Baton Rouge, LA, USA; ³Department of Radiology and Biomedical Imaging,
8 University of California, San Francisco, CA, USA; ⁴Graduate Program in Bioengineering,
9 University of California, Berkeley, CA, USA.

10 **Address Correspondence to:**

11 Steven B. Heymsfield, M.D.
12 Pennington Biomedical Research Center
13 6400 Perkins Rd.
14 Baton Rouge, LA 70808

15 **Tel:** 225-763-2541

16 **Fax:** 225-763-0935

17 **Email:** Steven.Heymsfield@pbrc.edu

18
19 **Number of text pages plus bibliography:** 19

20 **Tables:** 5

21 **Figures:** 5

22 **Running Title:** 3D System Comparisons

23 **Abbreviations:** 3D, three-dimensional; ADP, air-displacement plethysmography; CV,
24 coefficient of variation; DXA, dual-energy x-ray absorptiometry; SD, standard deviation.

25 **Key Words:** Body Composition; Anthropometry; Nutritional Assessment; Obesity.

26 **ABSTRACT**

27 **Background/Objectives:** Recent advances have extended anthropometry beyond flexible tape
28 measurements to automated three-dimensional optical devices that rapidly acquire hundreds of
29 body surface dimensions. Three new devices were recently introduced that share in common
30 inexpensive optical cameras. The design, and thus potential clinical applicability, of these
31 systems differ substantially leading us to critically evaluate their accuracy and precision.

32 **Subjects/Methods:** 113 adult subjects completed evaluations by the three optical devices (KX-
33 16 [16 stationary cameras], Proscanner [1 vertically-oscillating camera], and Styku scanner [1
34 stationary camera]), air displacement plethysmography (ADP), dual-energy x-ray absorptiometry
35 (DXA), and a flexible tape measure. Optical measurements were compared to reference method
36 estimates that included results acquired by flexible tape, DXA, and ADP.

37 **Results:** Optical devices provided respective circumference and regional volume estimates that
38 overall were well-correlated with those obtained from flexible tape measurements (e.g., hip
39 circumference: R^2 , 0.91, 0.90, 0.96 for the KX-16, Proscanner, and Styku scanner, respectively)
40 and DXA (e.g., trunk volume: R^2 , 0.97, 0.97, and 0.98). Total body volumes measured by the
41 optical devices were highly correlated with those from the ADP system (all R^2 s, 0.99).
42 Coefficient of variations obtained from duplicate measurements (n, 55) were larger in optical
43 than in reference measurements and significant ($p < 0.05$) bias was present for some optical
44 measurements relative to reference method estimates.

45 **Conclusions:** Overall, the evaluated optical imaging systems differing in design provided body
46 surface measurements that compared favorably with corresponding reference methods. However,

- 47 our evaluations uncovered system measurement limitations that with correction have the
- 48 potential to improve future developed devices.

49 INTRODUCTION

50 Anthropometry is an ancient method of quantifying human body size and shape.¹⁻³
51 Simple tools such as measuring rods and flexible calibrated tapes, calipers, and weight scales are
52 the traditional approaches whereby linear, circumferential, and mass estimates can be acquired as
53 part of nutritional assessment protocols.⁴⁻⁶ A relatively small number of somatic measurements
54 are now usually made by observers who ideally are well-trained and who are periodically
55 checked in quality control programs.^{7,8} Anthropometric methods, by not requiring ionizing
56 radiation for subject evaluation, are among the safest nutritional assessment approaches and are
57 widely used in pediatric^{9, 10} and pregnancy^{11,12} evaluations.

58 Rapid technological developments over the past decade are now revolutionizing
59 anthropometric approaches for assessing nutritional status. Imaging devices, ranging from two-
60 dimensional cellular telephone applications^{13,14} to three-dimensional (3D) whole-body laser
61 scanning systems¹⁵⁻¹⁷ can now quickly capture hundreds of body dimensions and with
62 appropriate software can provide numerous estimates of body size, shape, and composition.
63 While early systems, particularly those designed around laser technology,¹⁶ were costly and
64 primarily suitable for use in research settings, a new wave of relatively low-cost approaches is
65 appearing that have potential as clinical tools. One group of these new methods is based largely
66 on inexpensive optical depth cameras that were first introduced as components of gaming
67 systems.^{13,16-18}

68 These newer imaging approaches range in design from a potentially portable single
69 stationary camera coupled to a 360° rotating subject platform to a fixed array of 16 cameras that
70 surround the subject. With the emergence of several imaging methods, an important question

71 arises: do these differing approaches provide accurate and precise anthropometric measurements
72 comparable to those obtained by conventional laboratory-based reference methods? This is a
73 relevant question when applying these newer anthropometric devices to evaluate patients in the
74 clinical setting or subjects in research studies.

75 The aim of the current study was to critically evaluate three of these newer optical
76 devices differing in image acquisition and data processing technology by comparing body size
77 and shape results to those obtained by reference methods. Specifically, we compared device-
78 acquired circumferential and regional/whole body volume estimates to corresponding respective
79 estimates acquired with a flexible tape measure, dual-energy X-ray absorptiometry (DXA), and
80 air-displacement plethysmography (ADP).

81 **MATERIALS and METHODS**

82 **Experimental Design**

83 This was a cross-sectional study of an adult convenience sample. The study was approved
84 by the Pennington Biomedical Research Center Institutional Review Board and all subjects
85 signed an informed consent prior to participation.

86 Following screening and upon enrollment, each subject completed a baseline
87 questionnaire, including demographic information. They were then weighed and had their height
88 measured while clothed in a hospital gown. Anthropometric evaluations were then completed,
89 followed by DXA, ADP, and 3D imaging.

90 The collected data were used to compare 3D imaging system circumference, regional
91 body volume, and total body volume results between imaging devices and against reference
92 methods. Specifically, body circumferential estimates were obtained from 3D imaging and
93 conventional flexible tape-measure anthropometry; regional body volumes were obtained from
94 the 3D imaging devices and DXA; and total body volume estimates were made by the 3D
95 devices and ADP. The reference estimates for circumferences, regional volumes, and total
96 volumes were thus conventional flexible tape-measure anthropometry, DXA, and ADP,
97 respectively. Corresponding measurements from the imaging devices were compared to those
98 obtained by the reference methods.

99 **Participants**

100 Subjects were adult men and women volunteers at or over the age of 18 years. A pre-
101 evaluation screening questionnaire was used to ensure subjects were in good health and free of
102 chronic diseases. Subjects were recruited through advertisements on the center website. Once

103 enrolled, subjects were asked to arrive at the laboratory wearing or to change into form-fitting
104 clothing that included Spandex shorts and, for women, a Spandex top for all 3D scans and
105 anthropometric measurements. The same attire applied for ADP with the addition of a Lyrica cap
106 to cover loose hair. The DXA scan attire included only undergarments and an examination gown.

107 **Measurements**

108 Height was measured to the nearest 0.1 cm on each subject using a wall-mounted
109 stadiometer (Seca 222, Seca GmbH & Co. KG, Hamburg, Germany) and screening weight was
110 measured using a digital scale (MC-970; Tanita, Tokyo, Japan) to the nearest 0.1 kg. Each
111 measurement was evaluated twice with a third reading obtained if the first two respective
112 readings were >0.5 cm or >0.5 kg apart; results were averaged.

113 Anthropometric circumference measurements were taken by a trained staff member at the
114 anatomic locations used in the US National Health and Nutrition Examination Survey.¹⁹

115 Circumferences of the waist, hip, upper arms, and thighs were measured with a flexible tape and
116 recorded to the nearest 0.1 cm. Each measurement was taken three times and averaged. The
117 specific methods used in measuring these circumferences are presented in **Supplementary**

118 **Material.**

119 **3D Optical Scans**

120 **Image Acquisition.** Three imaging systems were used to obtain circumferences, regional
121 volumes, and total body volume. All three systems share in common the use of inexpensive,
122 consumer-grade optical depth cameras. With this feature in common, each device uses unique
123 mechanisms for capturing, assembling, and measuring the 3D subject images (**Figure 1** and
124 **Table S1**).

125 The KX-16 system (TC² Labs, Apex, NC) has four columns, each of which has four
126 evenly spaced Microsoft Kinect V1 cameras. The Kinect V1 sensor uses PrimeSense (Apple,
127 Inc., Cupertino, CA) technology. The columns are positioned in a rectangle and the subject
128 stands with their hands held in a downward V-shaped position, or “A-pose”, centered between
129 the columns during the 7-second scan. Each camera includes an infrared emitter that projects a
130 known pattern of points onto the scene. The infrared pattern is distorted by the subject and
131 imaged using an infrared sensor. The deformation of points is used to calculate depth.

132 The Proscanner (Fit3D, Redwood City, CA) uses a PrimeSense Carmine 1.08 depth
133 sensor that operates in the same way as the KX-16’s Kinect V1 sensors, although the
134 configuration of the system is different. The Proscanner uses one camera that oscillates vertically
135 on a tower while the subject rotates counterclockwise on a platform for about 40 seconds. The
136 subject tightly grips handlebars during the scan while their arms are held firmly in the A-pose.

137 The Styku scanner (Styku, Los Angeles, CA) also uses a single camera built into a tower
138 and a rotating platform to capture body image data. However, the Styku scanner uses a stationary
139 depth camera at a fixed height. The subject stands on the platform with their arms positioned in
140 the A-pose. The subject is then rotated clockwise for about 30 seconds. The Styku scanner uses a
141 Microsoft Kinect V2 camera that employs “time-of-flight” technology that is different from the
142 other systems. Infrared light is projected and reflected back to the sensor. The phase shifts in the
143 returning light waves are used to measure roundtrip light travel time that allows for a direct
144 calculation of depth.

145 **Image Processing.** The three systems use various iterative closest point²⁰ reconstruction
146 algorithms to create a 3D image. Over 250 measurement estimates of lengths, circumferences,

147 and volumes are calculated from the scan. Each system uses its own proprietary software for
148 landmark detection and measurement.

149 The Styku scanner displays a real-time depth video stream from the Kinect V2 sensor on
150 a computer screen while the subject rotates on the platform. As the subject rotates, the camera
151 captures new body views and uses Kinect Fusion software (Microsoft, Redmond, WA) to fuse
152 the depth data into a combined surface in real-time²¹ to produce a triangle mesh image. The
153 system then uses Poisson surface reconstruction methods to smooth and fill any surface holes.²²
154 Once the scan is complete, the Styku scanner's software is designed to recognize features found
155 on the mesh that are easily recognized body landmarks. From these features, a custom script
156 defines how the landmarks are used to calculate and visualize various body measurements. The
157 Styku scanner employs Graham's convex-hull algorithm²³ for refining circumference
158 measurements.

159 The TC² KX-16 and Fit3D Proscanner systems use image construction and measurement
160 techniques similar to those used by the Styku scanner. However, the Proscanner system software
161 does not fill in holes in the 3D mesh image while the KX-16 system fills in gaps at a few specific
162 regions such as under the arm. Neither scanner uses the surface smoothing algorithms
163 implemented by the Styku scanner.

164 **Dual-Energy X-Ray Absorptiometry**

165 Whole-body DXA scans were conducted using a Hologic Discovery A system with
166 Hologic Apex software version 40.2 (Hologic, Inc., Marlborough, MA). The completed scans
167 were evaluated for total body mass, regional mass (head, trunk, arms, legs), and body
168 composition (total and regional body fat, fat-free mass, lean soft tissue mass, and bone mineral

169 content). The regional mass cut-points were described earlier by Schuna et al.²⁴ Regional
170 volumes were estimated from their corresponding body composition estimates.²⁵

171 **Air Displacement Plethysmography**

172 Total body volume was measured with the Bod Pod ADP system (Cosmed USA,
173 Concord, CA). The volume of thoracic gas as quantified by the ADP system was not subtracted
174 from ADP total body volume estimates so as to be comparable to total volumes measured by the
175 three imaging systems.

176 An estimate of total body volume was available from DXA in addition to the reference
177 ADP method. DXA total body volume estimates were highly correlated with (**Supplementary**
178 **Figure S1**; $R^2=0.99$, $p<0.0001$) ADP estimates and there was no significant between-method
179 bias.

180 **Statistical Methods**

181 Four circumference measurements, five regional volumes, and total body volume
182 estimates from the 3D devices were compared to the corresponding reference method
183 measurements. At the outset we recognized that in some cases 3D system circumference and
184 regional volume measurements may not exactly match the anatomic sites as defined by the
185 reference methods. However, we did not know in advance to what extent these kinds of
186 differences might be present and their magnitudes. To explore the level of agreement between
187 3D optical and reference method measurements we examined if between-method group mean
188 differences were present, the magnitude of associations between the methods, and if between-
189 method bias was present.

190 Specifically, absolute circumference and volume estimates from the 3D optical devices
191 were compared to their reference method counterparts using paired t-tests with a difference of
192 $p < 0.05$ considered statistically significant. Associations between 3D optical and reference
193 method measurements were examined using linear regression analysis with statistical
194 significance set at $p < 0.05$. Bland-Altman plots were used to determine if significant 3D optical
195 measurement biases were present relative to the reference methods.

196 A subgroup of participants completed duplicate flexible tape, DXA, and 3D scans and the
197 respective coefficient of variations (CVs) expressed in % are presented in the results section. The
198 ADP CV for total body volume estimation is 0.1%.²⁶

199 Descriptive subject characteristics are presented as the mean \pm SD. Statistical analyses
200 were conducted using Microsoft Excel 2010 (Microsoft Corp., Redmond, WA) and GraphPad
201 Prism 7 (GraphPad Software Inc., La Jolla, CA).

202 RESULTS

203 Subjects

204 Subject characteristics are presented in **Table 1**. There were a total of 113 subjects (40
205 men, 73 women) ranging in age from 18 to 77 years and in BMI from 17.9 to 51.8 kg/m².

206 Coefficient of Variations

207 Fifty-five of the subjects completed duplicate flexible tape, DXA, and 3D optical scans
208 and the respective CVs are presented in **Table 2**. The flexible tape and DXA circumference and
209 volume CVs ranged from <1% to 1.5%. On average the 3D optical system CVs were larger, in
210 particular for the arm volume measurements (5.7, 3.9, 2.0, and 1.5% for KX-16, Proscanner,
211 Styku scanner, and DXA left arm, respectively).

212 Circumferences

213 Group averages for the circumferences are summarized in **Table 2**. The mean group
214 difference between the Styku scanner and flexible tape estimates for the representative hip
215 circumference (-0.02 cm) was not significant; significant mean hip circumference differences
216 were, however, present for the KX-16 (4.8 cm, p<0.0001) and Proscanner (1.2 cm, p<0.01). Root
217 mean square errors for the systems ranged from 2.6 for Styku scanner to 6.0 for the KX-16.

218 Circumference measurements by the 3D optical devices were all significantly correlated
219 with flexible tape measurements (R^2 s, 0.71-0.96, all p<0.0001)(**Table 2**). The representative hip
220 circumference measured by each system plotted against flexible tape measurements is shown in
221 **Figure 2** along with Bland-Altman plots. 3D and tape measurements were highly correlated

222 (R^2 s, 0.90-0.96, all $p < 0.001$). Significant hip circumference bias relative to the reference flexible
223 tape measurements was present for the Proscanner 3D system ($p < 0.01$).

224 **Regional Body Volumes**

225 Regional body volume results are summarized in **Table 2**. Representative trunk volumes
226 measured by the 3D systems were larger than DXA trunk volumes with mean differences of 10.4
227 L, 13.3 L, and 6.0 L for KX-16, Proscanner, and Styku scanner, respectively (all $p < 0.0001$). Of
228 these, the Styku scanner trunk volume estimates were the lowest of the three systems as they
229 were for all of the regional volume measurements. Root mean square errors for the systems
230 ranged from 6.4 for the Styku scanner to 14.0 for the Proscanner.

231 Regional volume measurements by the 3D optical devices were all significantly
232 correlated with DXA regional volume measurements (R^2 s, 0.69-0.98, all $p < 0.0001$)(**Table 2**).
233 Representative trunk volume estimates for the 3D systems are plotted against the DXA trunk
234 volume estimates in **Figure S2**. All of the 3D optical system estimates for trunk volume were
235 highly correlated with DXA trunk volume estimates (R^2 s ≥ 0.97 , $p < 0.0001$). Significant trunk
236 volume bias relative to the reference DXA measurements was present for all three optical
237 systems ($p < 0.0001$).

238 Following discussions with the investigators, the Fit3D Proscanner was updated by the
239 manufacturer to provide more significant figures for volume measurements after 80 subjects had
240 completed the study. The results display all 113 subjects for all measurements; however,
241 correlations for small regional volumes improved after the system update. Right arm volume for
242 the Proscanner vs. DXA is plotted from before the update and after the update in

243 **Supplementary Figure S3**.

244 **Total Body Volume**

245 The mean total body volume estimates were significantly different from those by ADP
246 for all three 3D optical systems ($p < 0.0001$)(**Table 2**). Root mean square errors for the systems
247 ranged from 2.9 for the Proscanner to 9.7 for the Styku scanner.

248 The results of linear regression and Bland-Altman analyses are displayed in **Table 2** and
249 **Figure S4** for each 3D optical system with ADP total volume as the reference. Total body
250 volumes determined by KX-16, Proscanner, and Styku scanners were highly correlated with
251 ADP volumes (R^2 s all 0.99). Bland-Altman plots all showed significant ($p < 0.05$) bias with
252 regression line slopes of -3.4 L, -2.4 L, and -9.1 L for the KX-16, Proscanner, and Styku scanner,
253 respectively. All of these slopes are negative indicating that that the 3D systems underestimated
254 body volume for larger subjects. As for regional volumes, the Styku system had the lowest total
255 body volume estimates for the three systems.

256

257 DISCUSSION

258 Three-dimensional optical imaging devices can provide hundreds of body surface
259 measurements in less than one minute. The full clinical potential of these many somatic surface
260 measurements has yet to be established. An initial step, the one taken in the current study, is to
261 determine the accuracy and precision of these optical devices relative to their reference method
262 counterparts. The aim of the current study was to evaluate three of these devices that share in
263 common inexpensive optical depth cameras but that differed in how these cameras are
264 configured and in data processing techniques.

265 Our findings overall indicate that all three of the evaluated systems provide reproducible
266 circumference, regional volume, and total body volume measurements that are well correlated
267 with the reference methods. Thus, even though the surface data acquisition hardware employed
268 by the systems differed, strong associations were observed between the optical device
269 measurements and those acquired with the reference methods. Critically evaluating what
270 technical concerns we did observe is illuminating with respect to these newly introduced
271 technologies.

272 Measurement Discrepancies

273 The first concern relates to absolute differences observed between 3D optical and
274 reference method landmarking. We were aware at the outset that optical-device measured
275 anatomic sites might not perfectly match those acquired by the reference methods, although the
276 magnitude of these discrepancies if present was unclear. At the current time there is no
277 standardization guideline adhered to by device manufacturers that states strict landmark
278 definitions. A main concern arising from this measurement inconsistency is that a subject's

279 results cannot be readily compared across systems or to standardized reference values. An
280 important consideration is that conventional anthropometric methods often rely on palpation of
281 boney landmarks for identifying measurement sites. By contrast, automated optical imaging
282 techniques discover measurement sites through identification of surface landmarks. The
283 possibility exists in future comparative studies to closer align measurement sites between
284 systems by application of surface markers prior to optical data acquisition. A similar approach
285 can be used to align 3D optical and DXA regional measurements.

286 Another source of absolute measurement differences is variation in the body regions
287 included in whole body volume estimates. We learned following completion of our analyses that
288 the KX-16 and Proscanner total body volume estimates do not include head, hands, or feet
289 volumes. By contrast, the Styku scanner includes these body parts in the total body volume
290 measurement. The CVs for 3D total body volume estimates were two or more times those by
291 ADP and DXA (**Table 2**) and when considered in light of the absolute measurement concerns it
292 is unlikely that optical devices at present can be used to accurately quantify body density and
293 thus body fat using the two compartment molecular level body composition model.²⁷

294 An absolute 3D-reference method difference may also have been caused by Styku
295 system's ToF technology that assumes light reflected from each pixel takes one path. In reality,
296 the geometry of the room or reflective surfaces in the room may cause light to take multiple
297 paths that are unpredictable and can alter the depth measurements.²⁸ The Styku scanner in our
298 study underestimated the distance between the platform and the sensor causing the measurements
299 to be systematically less than the reference values. While the recommended distance between the
300 platform and sensor still produced favorable correlations with reference methods, adjustments
301 could be made by changing the separation between the camera and platform and comparing

302 values to standard methods to determine optimal distance in a specific space. The system's
303 ability to track changes would not be affected if the system remains in the same position, but
304 could be if the system is moved.

305 Another source of measurement error may have resulted from subject characteristics. For
306 example, subjects who have a high BMI, are very tall, or who have poor balance may be
307 challenging to image. Thighs touching, as shown in the avatars created by the devices (**Figure**
308 **3**), may lead to errors when system landmarking software attempts to distinguish right from left
309 legs and legs from trunk. For subjects with a large amount of adipose tissue in the arms and
310 trunk, the upper extremities are difficult to distinguish from the trunk with the A-pose
311 implemented by all three systems and an arm may get cut off on KX-16 system avatars (**Figure**
312 **3**). These effects may partially explain why subjects who had a BMI within the normal range had
313 optical measurements closer to the reference method than those who were overweight or obese.
314 Additionally, some subjects were too tall for the Styku scanner and KX-16 cameras to capture
315 their full image. By contrast, the Proscanner's tower with mounted moving camera allowed for
316 greater total body imaging of tall subjects. Excluding a tall subject's head from the analysis can
317 lead to measurement bias as the head is a smaller proportion of body volume in people who tall
318 compared to those who are short.²⁴ The Styku scanner also requires subjects to stand still while
319 rotating with no arm support. Movement during the scan can cause malformed avatars (**Figure 3**)
320 that could affect measurement dimensions and CVs. Our recommendation is to do a quality
321 control check on all acquired 3D images before concluding the subject's evaluation.

322 **System Data Processing Differences**

323 While our focus was mainly on the automatically derived circumference and volume
324 measurements from each system, it should be noted that the 3D mesh processing and image
325 presentation varies between the systems. Reconstructed avatars display differences in resolution,
326 filling, and smoothing as shown in **Figure 3**. The Proscanner and KX-16 show minimal filling of
327 missing data and smoothing whereas the Styku scanner's image appears smooth with no gaps.
328 These differences do not appear to give any clear advantage in measurement quality since the
329 correlations and CVs were similar across the three systems.

330 A related data processing observation is that the Proscanner leg and arm volume
331 estimates were not well correlated with the DXA reference measurements at the start of the
332 study. In reviewing these observations we learned that the Proscanner did not provide an
333 adequate number of significant digits to allow for accurate measurement of small body segments.
334 We informed the manufacturer of this limitation and Fit3D developers subsequently added digits
335 to the results. Both the CVs and regional volume estimates improved accordingly (**Figure S3**).

336 **System Attributes**

337 Each system has distinct attributes such as cost, scan speed, and hardware design, but the
338 overall measurements compare similarly to reference methods. The Styku scanner's simple
339 design with a single fixed camera and modular design makes it easy to transport. The system also
340 displays results immediately and allows the user to interactively measure circumferences at any
341 point on the avatar. The Proscanner's moving camera allows capture of a tall subject's head
342 dimensions while the other systems do not include head measurements in tall subjects. The KX-
343 16 has the quickest scan time (7 sec), although this device is large and with 16 cameras is not
344 mobile and the system cost is higher than the other two devices.

345 Conclusions

346 The 3D optical systems evaluated in the current study that share in common inexpensive
347 image acquisition cameras provide reproducible circumference and volume measurements that
348 correlate well with reference methods that are often unavailable or too costly to apply in the
349 clinical setting. Our findings exposed important differences and limitations of these systems that
350 are largely correctible when building next generation devices. Future studies are needed to
351 establish the utility of these emerging optical devices in clinical and research settings.

352

353 Supplementary Information accompanies the paper on the EJCN website

354 (<http://www.nature.com/EJCN>)

ACKNOWLEDGEMENTS

The authors acknowledge the input provided by optical device manufacturers on the operational details of their respective systems.

FUNDING

This work was partially supported by two National Institutes of Health NORC Center Grants P30DK072476, Pennington/Louisiana; and P30DK040561, Harvard; and R01DK109008, Shape UP! Adults.

AUTHOR CONTRIBUTIONS

BB, CRS, LR, XL, BKN, JAS, and SBH analyzed the data and drafted the manuscript; BB, DL, CRS, LR, JAS, and SBH designed the study; BB, DL, CRS, and SBH directed implementation and data collection; BB, DL, CRS, and LR collected the data; LR, JAS, and SBH provided necessary logistical support; BB, DL, CRS, LR, XL, BKN, JAS, SBH edited the manuscript for intellectual content and provided critical comments on the manuscript.

CONFLICT of INTEREST

The authors declare no conflict of interest.

REFERENCES

1. FerroLuzzi A, Garza C, Haas J, Habicht DP, Himes J, Pradilla A *et al.* Physical status: The use and interpretation of anthropometry - Introduction. *Who Tech Rep Ser* 1995; **854**: 1-3.
2. Heymsfield SB, Stevens J. Anthropometry: continued refinements and new developments of an ancient method. *Am J Clin Nutr* 2017; **105**(1): 1-2. doi: 10.3945/ajcn.116.148346
3. Himes JH. *Anthropometric assessment of nutritional status*, Wiley-Liss: New York, 1991.
4. Cameron N. *The Measurement of Human Growth*, Croom Helm: London, 1984.
5. Madden AM, Smith S. Body composition and morphological assessment of nutritional status in adults: a review of anthropometric variables. *J Hum Nutr Diet* 2016; **29**(1): 7-25. doi: 10.1111/jhn.12278
6. Ulijaszek SJ, Mascie-Taylor CGN. *Anthropometry: The Individual and the Population* First edn, vol. 14. Cambridge University Press: Cambridge, 1994.
7. de Groot LC, Sette S, Zajkas G, Carbajal A, Amorim JA. Nutritional status: anthropometry. Euronut SENECA investigators. *Eur J Clin Nutr* 1991; **45 Suppl 3**: 31-42.
8. Lohman TG, Roche AF, Martorell R. *Anthropometric standardization reference manual*, Human Kinetics Books: Champaign, IL, 1988.
9. Frisancho AR. *Anthropometric standards for the assessment of growth and nutritional status*, University of Michigan Press: Ann Arbor, 1990.
10. Roche AF, Mukherjee D, Guo SM, Moore WM. Head circumference reference data: birth to 18 years. *Pediatrics* 1987; **79**(5): 706-712.
11. Paxton A, Lederman SA, Heymsfield SB, Wang J, Thornton JC, Pierson RN, Jr. Anthropometric equations for studying body fat in pregnant women. *Am J Clin Nutr* 1998; **67**(1): 104-110.

12. Piers LS, Diggavi SN, Thangam S, van Raaij JM, Shetty PS, Hautvast JG. Changes in energy expenditure, anthropometry, and energy intake during the course of pregnancy and lactation in well-nourished Indian women. *Am J Clin Nutr* 1995; **61**(3): 501-513.
13. Braganca S, Arezes PM, Carvalho M. An overview of the current three-dimensional body scanners for anthropometric data collection. In: Arezes PM, Baptista JS, Barroso MP, Carneiro P, Cordeiro P, Costa N *et al.* (eds). *Occupational Safety and Hygiene III*. CRC Press: Taylor & Francis Group: London, 2015, pp 149-154.
14. Capers PL, Kinsey AW, Miskell EL, Affuso O. Visual Representation of Body Shape in African-American and European American Women: Clinical Considerations. *Clin Med Insights Womens Health* 2016; **9**(Suppl 1): 63-70. doi: 10.4137/CMWH.S37587
15. Brooke-Wavell K, Jones PR, West GM. Reliability and repeatability of 3-D body scanner (LASS) measurements compared to anthropometry. *Ann Hum Biol* 1994; **21**(6): 571-577.
16. Soileau L, Bautista D, Johnson C, Gao C, Zhang K, Li X *et al.* Automated anthropometric phenotyping with novel Kinect-based three-dimensional imaging method: comparison with a reference laser imaging system. *Eur J Clin Nutr* 2016; **70**(4): 475-481. doi: 10.1038/ejcn.2015.132
17. Xie B, Avila JI, Ng BK, Fan B, Loo V, Gilsanz V *et al.* Accurate body composition measures from whole-body silhouettes. *Med Phys* 2015; **42**(8): 4668-4677. doi: 10.1118/1.4926557
18. Ng BK, Hinton BJ, Fan B, Kanaya AM, Shepherd JA. Clinical anthropometrics and body composition from 3D whole-body surface scans. *Eur J Clin Nutr* 2016; **70**(11): 1265-1270. doi: 10.1038/ejcn.2016.109
19. Centers for Disease Control and Prevention (CDC), National Center for Health Statistics (NCHS). National Health and Nutrition Examination Survey (NHANES): Anthropometry

- Procedures Manual. In: U.S. Department of Health and Human Services, Centers for Disease Control and Prevention, (eds). Hyattsville, MD: Centers for Disease Control and Prevention, 2007.
20. Method for registration of 3-D shapes. *Proc. SPIE 1611, Sensor Fusion IV: Control Paradigms and Data Structures*; April 30, 1992; Boston, MA, 1992.
 21. KinectFusion: real-time 3D reconstruction and interaction using a moving depth camera. *24th annual ACM symposium on User interface software and technology*; Oct. 16, 2011. ACM, 2011.
 22. Kazhdan M, Bolitho M, Hoppe H. Poisson surface reconstruction. In: Polthier K, Sheffer A (eds). *Eurographics Symposium on Geometry Processing*. The Eurographics Association, 2006, pp 61-70.
 23. Graham RL. An Efficient Algorithm for Determining the Convex Hull of a Finite Planar Set. *Information Processing Letters* 1972; **1**: 132-133.
 24. Schuna JM, Jr., Peterson CM, Thomas DM, Heo M, Hong S, Choi W *et al*. Scaling of adult regional body mass and body composition as a whole to height: Relevance to body shape and body mass index. *Am J Hum Biol* 2015; **27**(3): 372-379. doi: 10.1002/ajhb.22653
 25. Wilson JP, Mulligan K, Fan B, Sherman JL, Murphy EJ, Tai VW *et al*. Dual-energy X-ray absorptiometry-based body volume measurement for 4-compartment body composition. *Am J Clin Nutr* 2012; **95**(1): 25-31. doi: 10.3945/ajcn.111.019273
 26. Collins AL, McCarthy HD. Evaluation of factors determining the precision of body composition measurements by air displacement plethysmography. *Eur J Clin Nutr* 2003; **57**(6): 770-776. doi: 10.1038/sj.ejcn.1601609

27. Withers RT, Laforgia J, Heymsfield SB. Critical appraisal of the estimation of body composition via two-, three-, and four-compartment models. *Am J Hum Biol* 1999; **11**(2): 175-185. doi: 10.1002/(SICI)1520-6300(1999)11:2<175::AID-AJHB5>3.0.CO;2-C
28. Resolving multipath interference in kinect: An inverse problem approach. *IEEE Sensors 2014*. IEEE, 2014.

FIGURE LEGENDS

Figure 1. Configurations of the three optical imaging devices: KX-16 (left), Proscanner (center), Styku scanner (right). The Proscanner and KX-16 project patterns of infrared light on the subject and use light deformations to determine depth. The Styku scanner uses phase shifts in reflected waves to determine depth. The Styku scanner's camera's field of view is larger than that of the Proscanner and KX-16 (70.6 X 60 as opposed to 58.5 X 46.6).

Figure 2. Hip circumference measured by the 3D optical devices versus hip circumference estimates by a flexible tape measure and associated Bland-Altman plots. The solid line in each upper panel is the regression line and the dashed line is the line of identity.

Figure 3. Avatars from the KX-16 (A), Proscanner (B), and the Styku scanner (C). Images show system limitations such as arm cut off on the KX-16 (A), thighs touching on the Proscanner (B), and movement on the Styku scanner (C). The resolution is 320 X 240, 640 X 480, and 512 X 424 for the KX-16, Proscanner, and Styku scanner, respectively.

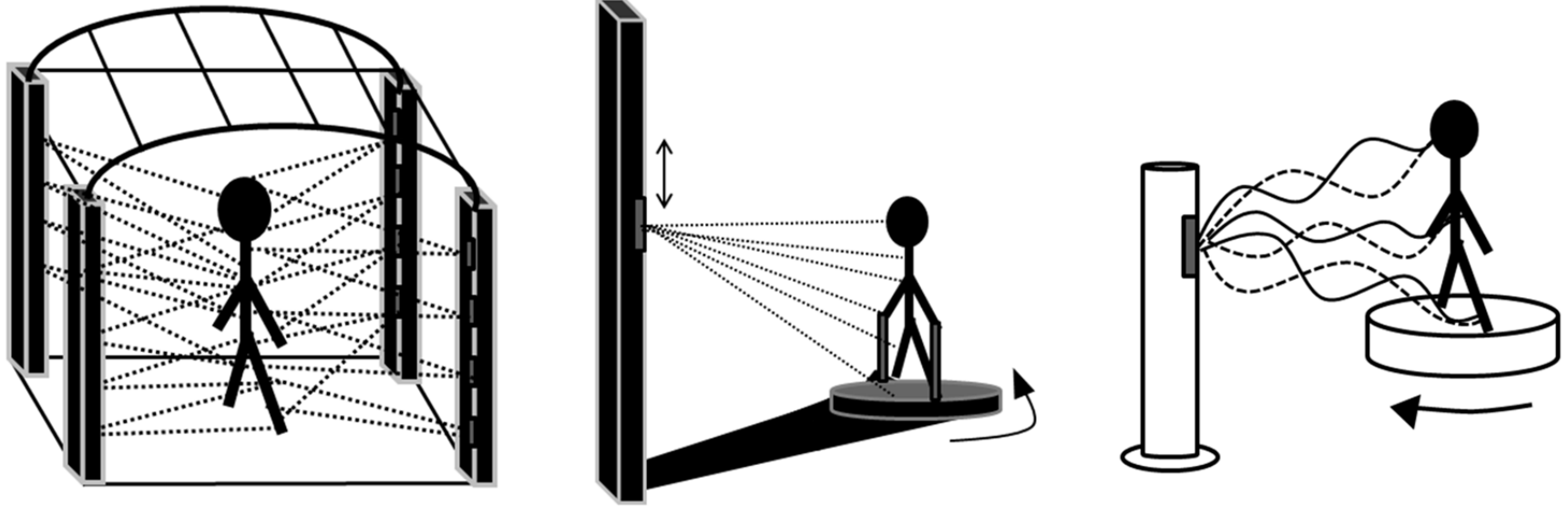


Figure 1

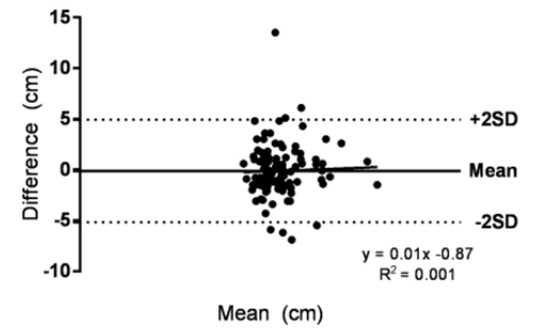
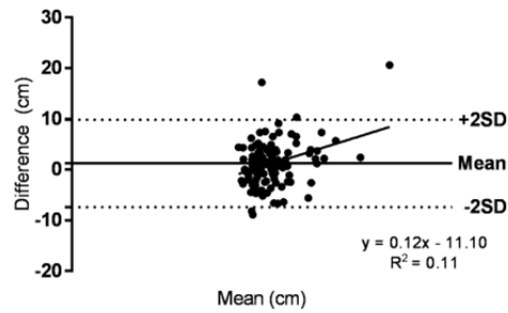
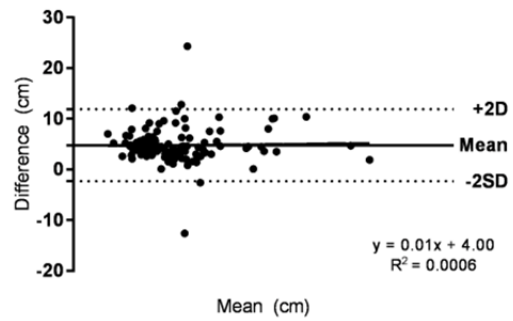
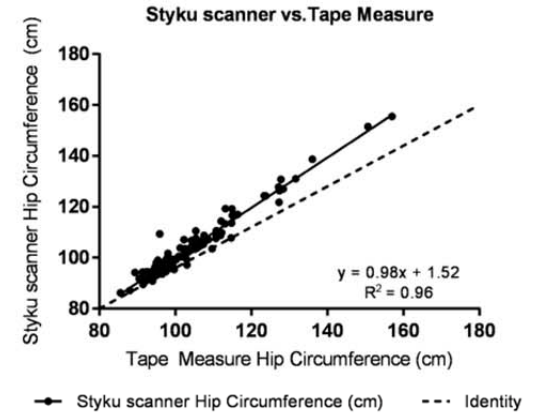
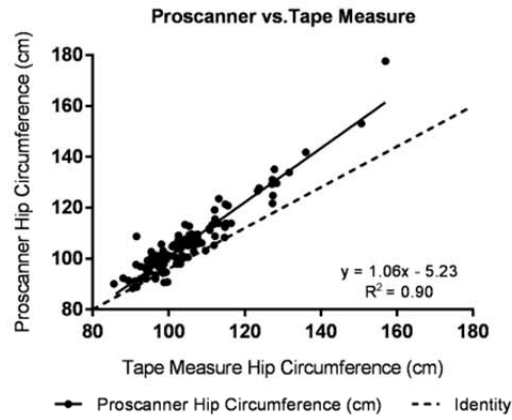
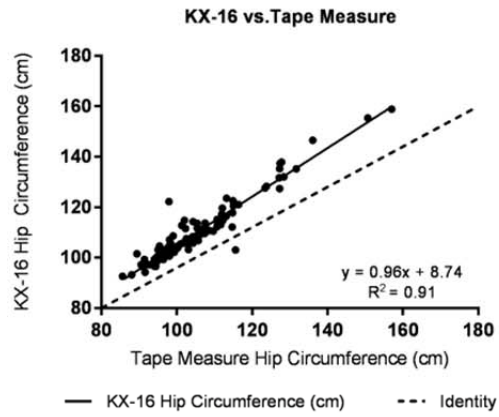


Figure 2

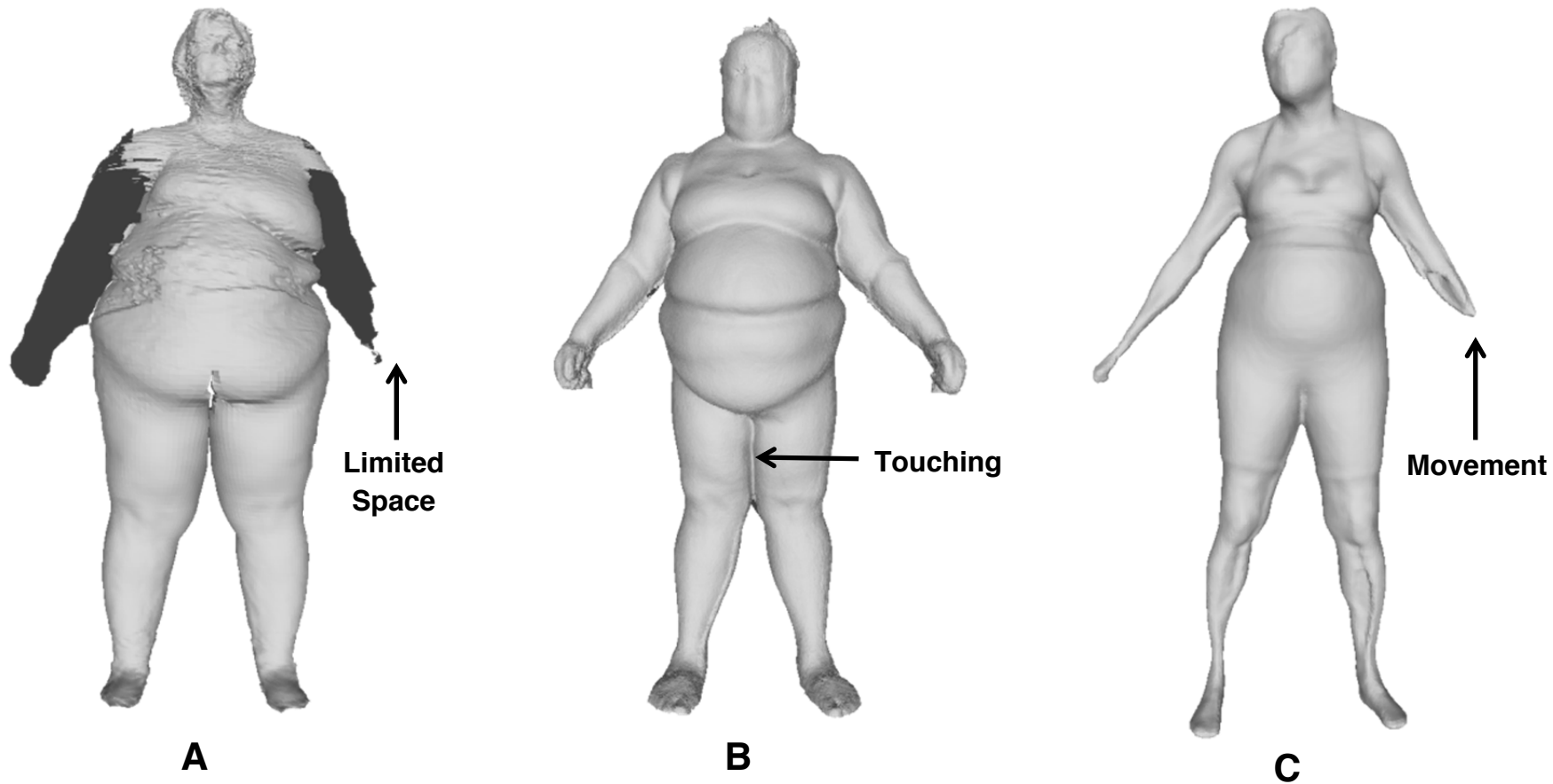


Figure 3

Table 1. Subject Characteristics.

	Men	Women
Number (White/Black/Asian)	40 (30/7/3)	73 (42/28/3)
Age (yrs)	41 ± 17	47 ± 17
Height (cm)	177.7 ± 6.4	163.0 ± 6.7
Weight (kg)	84.8 ± 17.0	73.4 ± 17.0
BMI (kg/cm ²)	26.7 ± 4.3	27.8 ± 7.0
% body fat †	22.3 ± 6.8	37.4 ± 7.8

Results are X±SD. Abbreviations: BMI, body mass index. †Acquired by DXA.

Table 2. Results of Circumference, Volume, and Coefficient of Variation Evaluations.

Measurement	Mean	Mean Δ	CV (%)	R ²	RMSE	Bland-Altman Analysis	
						R ²	Slope
Waist (cm)							
Tape Measure	89.6 ± 14.2		0.2 ± 0.1				
KX-16	90.2 ± 13.2	0.64	0.8 ± 0.8	0.86*	5.3	0.04 [‡]	-0.08
Proscanner	93.8 ± 14.1	4.21*	0.8 ± 1.2	0.92*	5.8	0.0005	-0.01
Styku scanner	84.5 ± 12.9	-5.08*	0.3 ± 0.4	0.94*	6.3	0.12 [†]	-0.10
Hip (cm)							
Tape Measure	105.0 ± 12.0		0.2 ± 0.3				
KX-16	109.8 ± 12.1	4.8*	0.4 ± 0.4	0.91*	6.0	0.0006	0.01
Proscanner	106.3 ± 13.3	1.2 [†]	0.4 ± 1.2	0.90*	4.6	0.11 [†]	0.12
Styku Scanner	104.9 ± 12.1	-0.02	0.1 ± 0.2	0.96*	2.6	0.001	0.01
Right Arm (cm)							
Tape Measure	33.2 ± 5.4		0.4 ± 0.2				
KX-16	35.9 ± 4.9	2.8*	2.6 ± 2.2	0.75*	3.9	0.05 [‡]	-0.12
Proscanner	33.2 ± 5.1	0.04	1.2 ± 1.0	0.87*	1.9	0.03	-0.07
Styku Scanner	29.1 ± 4.3	-4.1*	0.8 ± 1.3	0.73*	5.0	0.17*	-0.25
Right Thigh (cm)							
Tape Measure	56.8 ± 6.2		0.2 ± 0.1				
KX-16	63.0 ± 8.5	6.2*	0.9 ± 0.9	0.71*	7.7	0.27*	0.34
Proscanner	51.1 ± 5.5	-5.7*	0.7 ± 0.9	0.79*	6.4	0.06 [‡]	-0.12
Styku Scanner	57.3 ± 7.7	-0.2	0.3 ± 0.5	0.83*	3.3	0.24*	0.23
Body Volume (L)							
ADP	76.4 ± 18.3						
DXA	75.6 ± 18.1		0.2 ± 0.1				
KX-16	73.0 ± 16.9	-3.4*	0.8 ± 0.6	0.99*	4.2	0.31*	-0.08
Proscanner	74.0 ± 17.6	-2.4*	0.7 ± 0.6	0.99*	2.9	0.18*	-0.04
Styku scanner	67.4 ± 15.6	-9.1*	0.4 ± 0.4	0.99*	9.7	0.69*	-0.16
Trunk (L)							
DXA	36.4 ± 9.9		0.6 ± 0.5				
KX-16	46.8 ± 11.1	10.4*	1.0 ± 0.8	0.97*	10.7	0.31*	0.12
Proscanner	49.7 ± 13.5	13.3*	0.6 ± 0.9	0.97*	14.0	0.78*	0.31
Styku scanner	42.4 ± 11.0	6.0*	0.3 ± 0.3	0.98*	6.4	0.32*	0.11
Left Arm (L)							
DXA	4.3 ± 1.3		1.5 ± 1.2				
KX-16	3.6 ± 1.1	-0.7*	5.7 ± 4.4	0.82*	0.9	0.25*	-0.25
Proscanner	3.7 ± 1.1	-0.6*	3.9 ± 7.0	0.83*	0.8	0.23*	-0.23
Styku scanner	2.0 ± 0.6	-2.2*	2.0 ± 1.6	0.69*	2.4	0.73*	-0.83
Right Arm (L)							
DXA	4.5 ± 1.3		1.2 ± 1.2				
KX-16	3.7 ± 1.1	-0.7*	4.1 ± 3.0	0.87*	0.9	0.17*	-0.17
Proscanner	3.4 ± 1.1	-1.0*	2.1 ± 4.8	0.89*	1.1	0.21*	-0.17
Styku scanner	2.1 ± 0.6	-2.3*	2.4 ± 2.9	0.80*	2.5	0.79*	-0.76
Left Leg (L)							
DXA	13.0 ± 3.1		1.0 ± 0.8				
KX-16	9.3 ± 2.2	-3.69*	1.6 ± 1.7	0.90*	3.9	0.54*	-0.34
Proscanner	8.7 ± 1.7	-4.34*	2.4 ± 3.1	0.70*	4.8	0.61*	-0.64

Styku scanner	6.3 ± 1.6	-6.73*	0.8 ± 0.9	0.91*	7.0	0.85*	-0.65
Right Leg (L)							
DXA	13.1 ± 3.0		1.1 ± 0.7				
KX-16	9.6 ± 2.3	-3.55*	1.6 ± 1.8	0.90*	3.7	0.46*	-0.29
Proscanner	8.5 ± 1.6	-4.62*	1.5 ± 3.3	0.74*	5.0	0.62*	-0.65
Styku scanner	6.2 ± 1.6	-6.89*	1.4 ± 1.2	0.91*	7.1	0.84*	-0.62

Abbreviations: CV, coefficient of variation. RMSE, root means squared error. *, p<0.0001; †, p<0.01; ‡, p<0.05. Results are X±SD.

113 total subject evaluations for circumferences and volumes, 55 for coefficient of variations.